

# Intelligent Islanding Detection of Multi-distributed Generation Using Artificial Neural Network Based on Intrinsic Mode Function Feature

Samuel Admasie, Syed Basit Ali Bukhari, Teke Gush, Raza Haider, and Chul Hwan Kim

**Abstract**—The integration of distributed energy resources (DERs) into distribution networks is becoming increasingly important, as it supports the continued adoption of renewable power generation, combined heat and power plants, and storage systems. Nevertheless, inadvertent islanding operation is one of the major protection issues in distribution networks connected to DERs. This study proposes an intelligent islanding detection method (IIDM) using an intrinsic mode function (IMF) feature-based grey wolf optimized artificial neural network (GWO-ANN). In the proposed IIDM, the modal voltage signal is pre-processed by variational mode decomposition followed by Hilbert transform on each IMF to derive highly involved features. Then, the energy and standard deviation of IMFs are employed to train/test the GWO-ANN model for identifying the islanding operations from other non-islanding events. To evaluate the performance of the proposed IIDM, various islanding and non-islanding conditions such as faults, voltage sag, linear and nonlinear load and switching, are considered as the training and testing datasets. Moreover, the proposed IIDM is evaluated under noise conditions for the measured voltage signal. The simulation results demonstrate that the proposed IIDM is capable of differentiating between islanding and non-islanding events without any sensitivity under noise conditions in the test signal.

**Index Terms**—Distributed energy resource (DER), intrinsic mode function (IMF), grey wolf optimized artificial neural network (GWO-ANN), intelligent islanding detection method (IIDM), microgrid.

## I. INTRODUCTION

THE integration of distributed energy resources (DERs) to the existing distribution networks is highly important owing to deregulated energy market policies, global issues,

and the advancement of modern power systems in the form of smart grids [1] - [4]. Nevertheless, interconnected DERs are subject to inadvertent islanding operation, which, if undetected, may cause various issues such as unregulated voltage and frequency, as well as resynchronization and out-of-phase reclosing problems, and may also endanger maintenance personnel [5]-[7]. Inadvertent islanding is a condition in which the power from the utility system is lost, but the islanded DERs continue to supply power locally to a fragment of the distribution network. However, current standards such as IEEE 1547 [8] and UL-1741 [9] have recommend that the islanded DERs should be promptly ceased. Therefore, effective islanding detection is the most critical requirement in the integration of DERs to the distribution network [10], [11].

To date, islanding detection is an open research problem in grid integration and many researchers brought various islanding detection approaches. The islanding detection approaches can be broadly divided into remote and local [12]. Remote islanding detection approaches are based on the communication between the utility system and DERs, so that trip signal is initiated to DERs when islands are formed. They are effective, fast and accurate, but require a communication infrastructure. Hence, they are uneconomical, particularly for small-scale units [13]. As a result, local islanding detection approaches, specifically the practical schemes based on monitoring grid parameters at the point of connection (PoC) of DER, are gaining preference over remote approaches.

The local islanding approaches are further categorized into active, passive, and hybrid. Active islanding detection methods (IDMs) are based on injecting a small external disturbance signal and monitoring the consequent response signal [14]. The main advantage of active IDMs is their small non-detection zone (NDZ). However, these schemes are complex and have an adverse effect on the normal operation of the DER system owing to the injected disturbance signal. Furthermore, they malfunction in multi-DER systems due to mutual interference effects and the cancelation of injected perturbations [15]. Passive IDMs rely on continuously monitoring the relative variation of grid parameters at the targeted DERs [16]-[18]. These schemes are fairly simple to implement without any power quality issues. However, their NDZs are prominent, particularly for small power mismatch between the generation and load. On the other hand, considering the advantages of both active and passive IDMs, hy-

Manuscript received: April 16, 2019; accepted: November 5, 2019. Date of CrossCheck: November 5, 2019. Date of online publication: April 9, 2020.

This work was supported by the National Research Foundation (NRF) of South Korea funded by the Ministry of Science, ICT & Future Planning (MSIP) of the Korean government (No. 2018R1A2A1A05078680).

This article is distributed under the terms of the Creative Commons Attribution 4.0 International License (<http://creativecommons.org/licenses/by/4.0/>).

S. Admasie, S. B. Ali Bukhari, T. Gush, R. Haider, and C. H. Kim (corresponding author) are with the Department of Electrical and Computer Engineering, Sungkyunkwan University, Suwon, South Korea. S. B. Ali Bukhari is also with the U.S.-Pakistan Center for Advanced Studies in Energy (USPCAS-E), National University of Sciences and Technology (NUST), H-12 Islamabad, Pakistan, and R. Haider is also with the Department of Electrical Engineering, Balochistan University of Engineering and Technology, Khuzdar 89100, Pakistan (e-mail: sami2018@skku.edu; basit@uspcase.nust.edu.pk; gushteke@skku.edu; razahaider@buetk.edu.pk; chkim@skku.edu).

DOI: 10.35833/MPCE.2019.000255



brid schemes have also been proposed to detect islanding using active schemes when the passive ones suffer NDZ [16], [19], [20]. However, hybrid active and passive schemes are complex and inefficient. Furthermore, their NDZs and the requirements to set appropriate threshold value are the major limitations of the existing IDMs under conditions of near-zero power mismatch between generation and islanded loads. Setting an appropriate threshold value for signal processing based IDMs is highly challenging, as lower threshold values may reduce the ride-through capability, whereas a higher threshold may lead to the delayed detection of islanding events.

The state-of-the-art technique for alleviating the threshold and NDZ problems in islanding detection is a combination of signal processing and intelligent classifiers. Signal pre-processing is used to derive important features of the input test signal. Then, intelligent classifiers are used to train and build a model for islanding classification based on the features of the test signal. The Fourier and the short-time Fourier transforms are the most widely-used simple feature extraction techniques in signal processing. However, these schemes have low time-frequency resolutions. As a result, the techniques of time-frequency multi-resolution analysis such as the wavelet transform, the Stockwell transform, and empirical mode decomposition, have recently been proposed in power signal processing for power quality disturbance, fault, and islanding detection [21]–[24]. Machine learning classifiers are promising approaches to mitigate the threshold issues in passive IDMs that rely on signal processing. These schemes learn from the time-frequency feature data to detect the islanding operation. In [25], islanding detection is proposed based on learning data using support vector machine (SVM). However, both current and voltage data are required, which is computationally expensive. The ANN-based islanding detection method is employed in [26], which is capable of identifying islanding operations only based on the samples of voltage waveforms extracted from DER ends. However, it does not consider the multiple types of DERs. In the proposed intelligent IDM (IIDM), the statistical features of intrinsic mode functions (IMFs) at the PoC of the targeted DERs are used as input to a grey wolf optimized artificial neural network (GWO-ANN) to determine whether DERs operate in grid-connected or islanded mode.

In brief, this study contributes to the state-of-the-art approaches with the following key contributions:

- 1) A GWO-ANN model is proposed for islanding detection to mitigate the difficulty in setting appropriate threshold values of signal processing based IDMs.
- 2) An IMF feature based IIDM applicable to hybrid DER systems benchmarked is proposed with two inverter-based (IVB) and two synchronous-machine-based (SMB) DERs.
- 3) Considering the non-islanding and islanding events, which commonly happen, an IIDM with classification accuracy of 99.5% is proposed with perfectly matched power between the generation and load.

The remainder of this paper is organized as follows. In Section II, the proposed IIDM is described. The GWO-ANN

based classifier is illustrated in Section III. Section IV presents the data set generation used to develop the proposed IIDM. In Section V, the simulation results and performance analysis of the proposed IIDM are presented. Finally, Section VI concludes the paper and provides directions for future work.

## II. DESCRIPTION OF PROPOSED IIDM

An IIDM using IMF feature based GWO-ANN is proposed for detecting and distinguishing islanding operation from other non-islanding events. Figure 1 shows a flowchart of the proposed IIDM. Initially, a three-phase voltage signal at the PoC of the targeted DERs is retrieved and transformed into a modal signal, which eventually mitigates the computation and memory requirement for processing the raw three-phase signal. Subsequently, the five-cycle modal signal is processed through variational mode decomposition (VMD) to obtain narrow-banded IMFs. Finally, the energy and the standard deviation of each IMF are extracted and used as inputs to the GWO-ANN classifier.

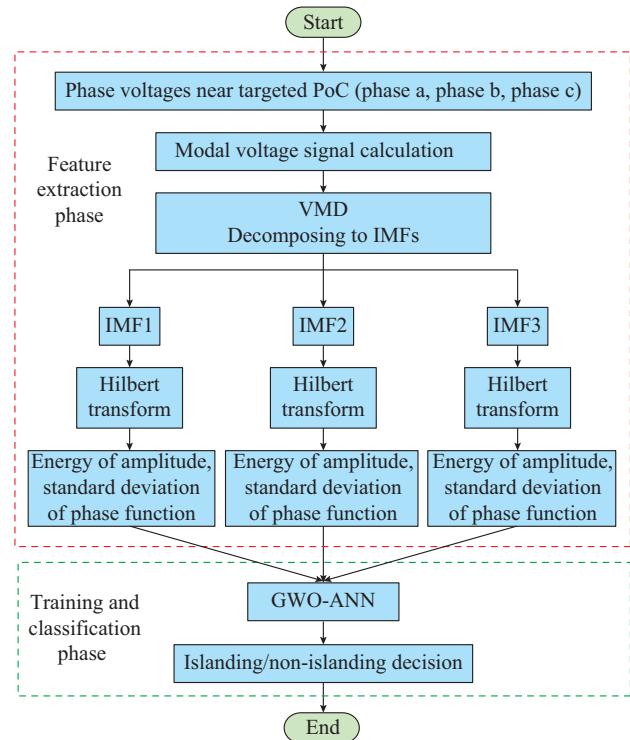


Fig. 1. Flowchart of proposed IIDM.

### A. Test System

A single-line diagram of the studied system is shown in Fig. 2. The test system is a grid-connected microgrid containing multiple types of DERs (both IVB and SMB). It operates at 25 kV/60 Hz and is interconnected to the utility system within a 500 MVA short-circuit capacity bus through a 125 kV/25 kV distribution transformer. The system consists of two IVB-DERs ( $2 \times 6$  MVA = 12 MVA), two SMB-DERs ( $2 \times 9$  MVA = 18 MVA), buses (B), main grid, step-down transformers (T), circuit breakers (CB), and local loads. To

evaluate the proposed IIDM, five islanded areas (IA\_1, IA\_2, IA\_3, IA\_4, IA\_5) are outlined in Fig. 2. The components of the system are modelled in the MATLAB/Simulink environment and detailed in [27].

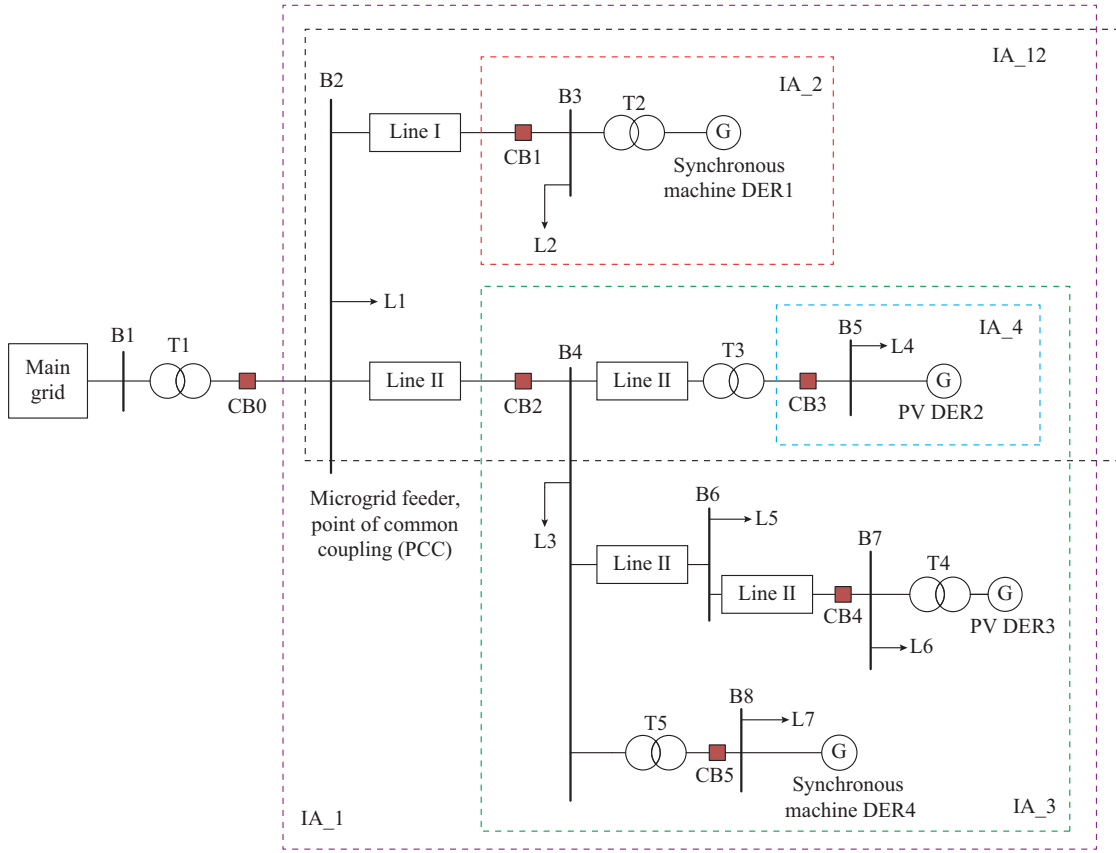


Fig. 2. Test system under study.

### B. Signal Pre-processing

The three-phase voltage signals at the targeted bus are sampled at 3.84 kHz (64 samples per cycle). To mitigate the computation time and memory requirement of per-phase analysis, a transformed modal signal is taken as input to the VMD model. The modal signal is given by:

$$V_m = \alpha V_a + \beta V_b + \gamma V_c \quad (1)$$

where  $V_m$  is the modal signal;  $V_a$ ,  $V_b$  and  $V_c$  are the voltages of phases a, b and c, respectively; and the coefficients  $\alpha$ ,  $\beta$  and  $\gamma$  are the transformation quantities set to be 1, 2 and -3, respectively [28], [29].

### C. Feature Extraction Using Voltage Signal IMFs

Time-frequency feature extraction is a fundamental task for accurate detection and classification of disturbance events. In the proposed method, a VMD is used to perform a time-domain filter analysis based on the measured modal voltage signal. The application of VMD technique to monitor the dynamic patterns of the modal voltage signal for islanding detection purpose is firstly introduced in [30]. VMD decomposes the non-stationary modal voltage signal into a series of band-limited IMFs, which are oscillatory signals that have variable amplitude and frequency as a function of

time expressed as follows [31]:

$$u_k(t) = \sum_k A_k(t) \cos(\phi_k(t)) \quad (2)$$

where  $u_k(t)$  is the mode function;  $\phi_k(t)$  is the phase; and  $A_k(t)$  is the envelope of the oscillatory sub-signals. The VMD algorithm is a constrained variational optimization problem defined as:

$$\begin{cases} \min_{\{u_k\}, \{w_k\}} \left\{ \sum_{k=1}^K \left\| \partial_t \left( \delta(t) + \frac{j}{\pi t} \right) u_k(t) e^{-jw_k t} \right\|_2^2 \right\} \\ \text{s.t. } \sum_{k=1}^K u_k = f \end{cases} \quad (3)$$

where  $\delta(t)$  is the Dirac delta function;  $K$  is the number of modes to be involved in the decomposition process, which is chosen prior to the optimization routine;  $\partial_t$  is the derivative with respect to  $t$ ;  $\|\cdot\|_2^2$  is the square of the  $L^2$ -norm;  $\{u_k\} = \{u_1, u_2, \dots, u_K\}$  and  $\{w_k\} = \{w_1, w_2, \dots, w_K\}$  are the sets of all modes and their center frequencies, respectively; and  $f$  is the input signal. The constrained variational problem is equivalently represented as an unconstrained optimization problem by further introducing a quadratic penalty  $\lambda$  and a data fidelity parameter  $\chi$  as:

$$\ell(u_k, w_k, \lambda) = \chi \left\{ \sum_{k=1}^K \left\| \partial_t \left( \delta(t) + \frac{j}{\pi t} \right) u_k(t) e^{-jw_k t} \right\|_2^2 \right\} + \left\| f - \sum_{k=1}^K u_k \right\|_2^2 + \left\langle \lambda, f - \sum_{k=1}^K u_k \right\rangle \quad (4)$$

where  $\langle \cdot \rangle$  denotes the inner product. Afterwards, the alternate direction method of multipliers (ADMM) solves the unconstrained optimization problem by converting the original complex optimization problem into sub-optimization problems [31]. The solution in the spectral domain is:

$$\hat{u}_k = \frac{\hat{f}(w) - \sum_{i \neq k} \hat{u}_i(w) + \hat{\lambda}(w)/2}{1 + 2\alpha(w - w_k)^2} \quad (5)$$

where  $\hat{u}_k$ ,  $\hat{f}(w)$  and  $\hat{\lambda}(w)$  are the mode function, input function and Lagrangian multiplier in the spectral domain, respectively.  $\sum_{i \neq k} \hat{u}_i(w)$  is the sum of intrinsic mode functions that may be present in the signal but not extracted in  $\hat{u}_k$ . Weiner filtering is used for mode updating in the VMD algorithm. Specifically, the Wiener filter is tuned to its center frequency  $w_k^n$ . The corresponding ADMM mode updating process for iteration count  $n+1$ , for all modes from  $k=1$  to  $K$ , is given as follows:

$$\hat{u}_k^{n+1} = \frac{\hat{f}(w) - \sum_{i=1}^{k-1} \hat{u}_i^{n+1}(w) - \sum_{i=k+1}^K \hat{u}_i^n(w) + \hat{\lambda}^n(w)/2}{1 + 2\alpha(w - w_k^n)^2} \quad (6)$$

Similarly, the following equation is used to update the center frequencies:

$$w_k^{n+1} = \frac{\int_0^\infty w |\hat{u}_k^{n+1}(w)|^2 dw}{\int_0^\infty |\hat{u}_k^{n+1}(w)|^2 dw} \quad (7)$$

The iterations in mode and central frequency updating continue until the following stopping criterion is satisfied:

$$\sum_k \frac{\|\hat{u}_k^{n+1} - \hat{u}_k^n\|_2^2}{\|\hat{u}_k^n\|_2^2} < \varepsilon \quad (8)$$

where  $\varepsilon = 1 \times 10^{-5}$  is used in this study.

As the initial IMFs are carrying the dominant modes following a disturbance, the first three IMFs are considered for feature extraction [32], [33]. Afterwards, these IMFs are further processed using Hilbert transform and then the two statistical features, energy and standard deviation of each IMFs are calculated. Let  $v_k(t)$  be the Hilbert transform of IMF  $u_k(t)$ , then the analytic signal can be given by:

$$z_k(t) = u_k(t) + iv_k(t) \quad (9)$$

where  $v_k(t)$  is the actual Hilbert transform of the IMF signal, which is computed by the convolution of the function  $1/(\pi t)$  with the function  $u_k(t)$ :

$$H(u_k(t)) = \frac{1}{\pi} P \int_{-\infty}^{\infty} \frac{u_k(\tau)}{t - \tau} d\tau \quad (10)$$

where  $P$  denotes the Cauchy principal value, which extends the class of functions for which the integral in (10) exists. For a non-stationary signal whose spectral content varies

with time, the instantaneous amplitude and frequency play an important role in the understanding of its characteristics [34], [35]. The instantaneous amplitude and phase of the analytic signal are calculated as:

$$M_k(t) = \sqrt{u_k^2(t) + v_k^2(t)} \quad (11)$$

$$\theta_k(t) = \arctan \frac{v_k(t)}{u_k(t)} \quad (12)$$

Eventually, the energy content and standard deviation of the amplitude and actual HT of the IMF signal are computed and used as an input feature to train and classify the islanding events, respectively.

### III. GWO-ANN CLASSIFIER

Currently, machine learning algorithms are extensively used for classification of power quality disturbances and faults owing to their capability to handle large sets of data, and their potential to eliminate threshold calculations [36], [37]. The proposed IIDM is based on the hypothesis that the targeted PoC voltage measurements can immediately indicate islanding operation after proper training of the machine learning model. In conventional ANNs, a training rule is recursively applied in each layer. Thereby, the contribution of each weight to the total error is calculated reversely from the output layer back to the input layer, and then the gradient descent algorithm is used to optimize the weights and biases.

Improper classification, slow convergence, and the trapping in local minima are the disadvantages of conventional ANNs. In contrast, recent stochastic optimization ANNs such as particle swarm optimization, ant colony optimization, genetic algorithms, and GWO-based ANNs, start the training process with a random solution(s) and evolve it (them) [38]-[41]. Recently, meta-heuristic optimization techniques have attracted wide attention, because with few parameters, they are simple to be used in challenging problems to avoid local optimal solution, and are flexible as well as derivation-free [42], [43]. Moreover, GWO algorithms have the so-called  $\alpha$  class, which can be used to overcome the drawbacks of other schemes of swarm intelligence optimization.

The variables to be optimized in the ANN are weights and biases. Therefore, the dimension of the optimization problem is equal to the total number of weights and biases (thresholds) in the ANN model. Accordingly, the objective of GWO-ANN is to find a set of optimal weights and biases that maximize the classification accuracy for both training and testing data sets. The overall process of the proposed model is shown in the schematic diagram given in Fig. 3. The performance of the classifier is evaluated using the average mean square error (MSE):

$$MSE = \frac{1}{l} \sum_{i=1}^l (o_m - d_m)^2 \quad (13)$$

where  $l$  is the number of training data sets; and  $o_m$  and  $d_m$  are the actual and desired outputs when the  $m^{\text{th}}$  training input is used, respectively. It is noted that  $b_i$  ( $i=1, 2, \dots, l$ ) in Fig. 3 are the biases of the hidden neurons in the given



ANN model.

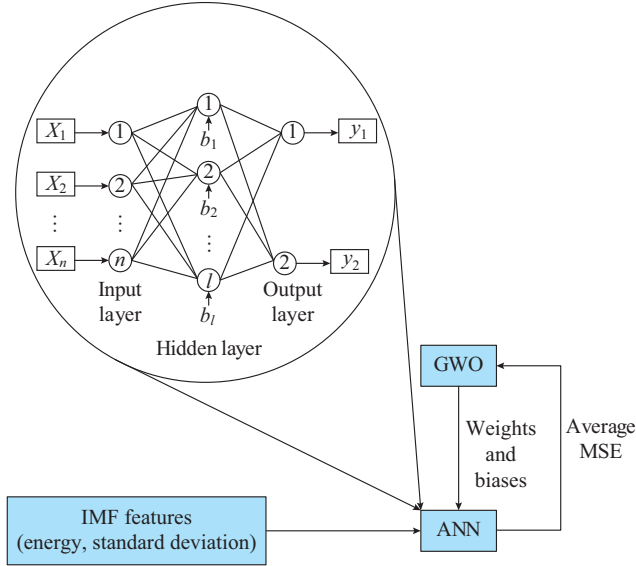


Fig. 3. GWO-ANN model.

#### IV. DATASET GENERATION

##### A. Case Studies for Performance Analysis of Proposed IIDM Under Islanding Conditions

Islanding cases are generated with varying active and reactive power mismatches from  $-50\%$  to  $50\%$  and  $-20\%$  to  $20\%$ , respectively, which are used as input features to train and test the model. The feature vectors represent the energy and standard deviation of the voltage signal IMFs. These feature vectors are used to train and test the GWO-ANN model to classify islanding and non-islanding events. The simulated events include 1344 islanding (positive) and 672 non-islanding (negative) events. Table I summarizes the status of the CBs for various islanding scenarios.

TABLE I  
STATUS OF CBS FOR ISLANDED CASES

| Islanded region | Status of CBs |        |        |        |
|-----------------|---------------|--------|--------|--------|
|                 | CB0           | CB1    | CB2    | CB3    |
| IA_1            | Open          | Closed | Closed | Closed |
| IA_2            | Closed        | Open   | Closed | Closed |
| IA_3            | Closed        | Closed | Open   | Closed |
| IA_12           | Closed        | Open   | Open   | Closed |

##### 1) Islanding Considering Only IVB DERs

The islanding operation of only IVB DERs are simulated by switching CB3 at  $t=0.5$ s to make the region shown in IA\_4. A total of 441 islanding events are recorded at bus B5, with  $-50\%$  to  $50\%$  active and  $-20\%$  to  $20\%$  reactive power mismatches. The performance of islanding detection during IVB islanding operation is examined for normal and noisy data by introducing a signal noise ratio (SNR) value of 35 dB to the training and testing datasets.

##### 2) Islanding Considering Only SMB DERs

Similarly, the proposed IIDM is evaluated for islanding

operation of SMB DERs. In this case, DER1 connected to bus B3 in IA\_2 region is islanded to test the proposed IIDM. The islanding operation of DER1 is simulated by switching CB1 at  $t=0.5$  s. The total number of datasets collected during islanding operation of IA\_2 is 231, with 320 samples each.

##### 3) Islanding Considering Multi-DERs

To study the effect of both IVB and SMB islanding DERs on the performance of the proposed IIDM, an islanding condition is created in the lower stream feeders of the grid-connected microgrid by switching CB0 at  $t=0.5$  s, and thus all IVB and SMB DERs are islanded. The voltage signals at the PCC are measured and processed to be the input for the GWO-ANN classifier. Sample IMFs including their instantaneous amplitude of the analytic function during multi-DER islanding at  $\Delta P=-50\%$  and  $\Delta Q=-20\%$  are shown in Figs. 4 and 5, respectively, where  $\Delta P$  and  $\Delta Q$  are the mismatch active and reactive power between the generation and load in the islanded region, respectively.

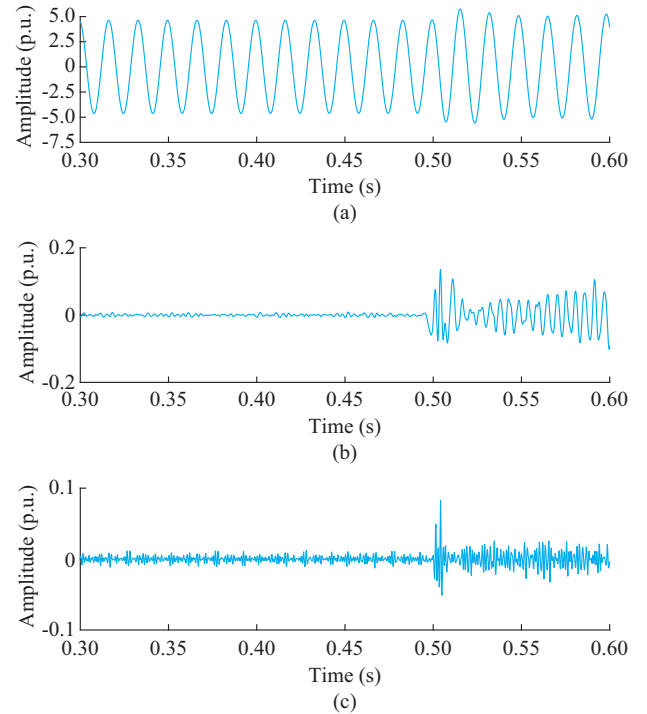


Fig. 4. IMFs of modal signal measured at PCC during islanding considering multi-DERs. (a) IMF1. (b) IMF2. (c) IMF3.

##### B. Case Studies for Performance Analysis of Proposed IIDM Under Non-islanding Conditions

To evaluate the performance of the proposed IIDM in discriminating islanding and non-islanding events, four cases are considered in training and testing the GWO-ANN classifier model. They include both linear and non-linear load switching, capacitive switching, and the information of fault event time-frequency, which are input to the classifier model. The non-islanding datasets contain 672 modal signals with 320 samples each, retrieved from the PoC of voltage measurements of targeted DERs.

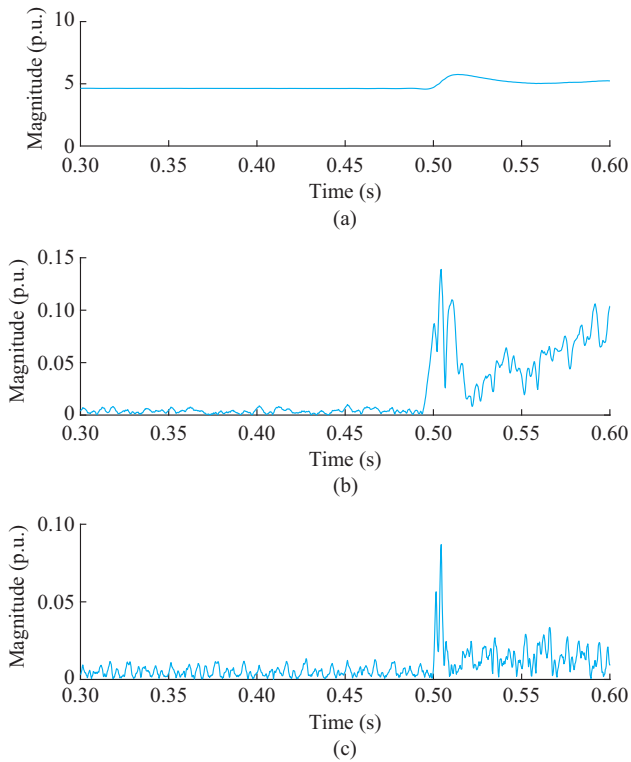


Fig. 5. Instantaneous amplitude of analytic function for IMFs during islanding considering multi-DERs. (a) M1. (b) M2. (c) M3.

### 1) Impact of Load Switching

To examine the proposed IIDM for component switching events, linear and non-linear load switching and capacitor switching are considered. The switching of a capacitive load leads to transient variations of the grid parameters. Therefore, capacitor switching events may affect the islanding detection scheme. To evaluate the effect of capacitor switching on islanding detection, various data sets with capacitor switching are used at different buses in the training and testing of the GWO-ANN model. The capacitor banks are disconnected at  $t=0.5$  s to monitor the effect of capacitor switching from 10 kvar to 100 kvar at different buses. A total of 85 load switching events are generated by connecting and disconnecting both linear and non-linear loads in the distribution network. For brevity, the IMFs for capacitor bank switching connected to the feeder of microgrid are illustrated. Figures 6 and 7 show the IMFs and their instantaneous amplitudes of the analytic functions for a sample capacitor switching event at the PCC.

### 2) Effect of Fault Events

Grid fault is one of the most common disturbances in power systems that may affect islanding detection. Effective islanding detection schemes should discriminate the islanding events from such grid disturbances to eliminate the false tripping of DERs in an integrated distribution network. To investigate the effect of fault events in the proposed IIDM, the common fault types on B2, i.e., single-line-to-ground, double-lines-to-ground (LLG), and three-lines-to-ground (LLLG) faults with variable fault resistance are considered in the

training and testing phase of GWO-ANN. In recording the fault data, all fault events (597 fault cases) are triggered at  $t=0.5$  s and a five-cycle post-fault data is retained for variable fault resistance.

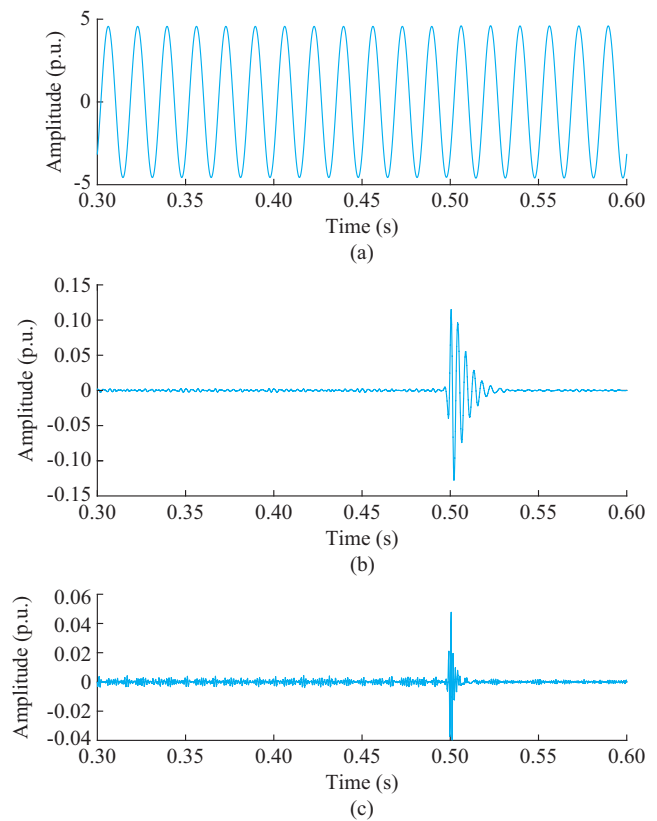


Fig. 6. IMFs of modal signal measured at PCC during capacitive load switching. (a) IMF1. (b) IMF2. (c) IMF3.

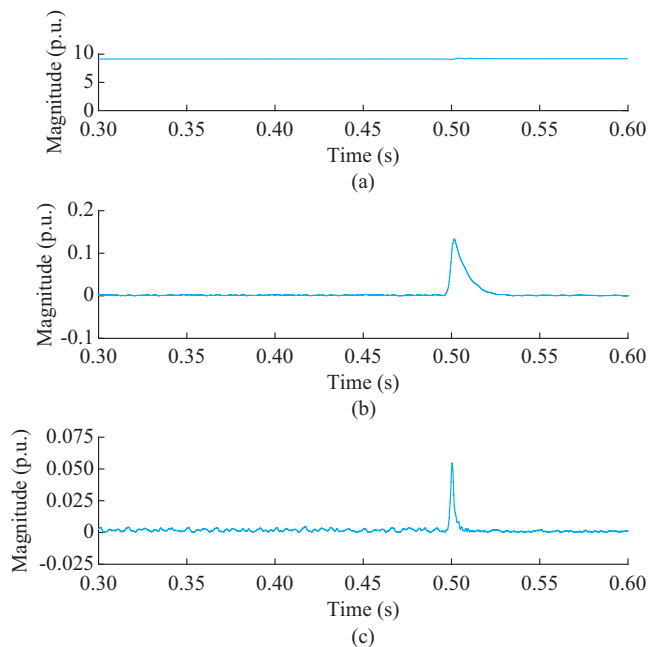


Fig. 7. Instantaneous amplitude of analytic function for IMFs during capacitive load switching. (a) M1. (b) M2. (c) M3.

V. RESULTS AND DISCUSSION

To investigate the performance of the proposed IIDM, a set of islanding classification metrics were defined. These statistical metrics are important indexes employed to assess the performance of various intelligent islanding detection schemes [27], [44]. The first performance metric is used to measure the performance against early detection or nuisance tripping. It is called precision, and is defined as the ratio of

predicted islanding events to the sum of predicted islanding events and non-islanding events wrongly predicted as islanding. Table II shows that the proposed IIDM is not susceptible to false detection of islanding events. Moreover, to measure the performance against delayed detection, a metric called dependability is used. It is defined as the ratio of predicted islanding events to the sum of islanding events and islanding events wrongly predicted as non-islanding.

TABLE II  
PERFORMANCE ANALYSIS OF PROPOSED IIDM AGAINST NUISANCE TRIPPING

| Run     | Precision during islanding of multi-DERs (%) |           | Precision during islanding of IVB DERs (%) |           | Precision during islanding of SMB DERs (%) |           |
|---------|--|-----------|--|-----------|--|-----------|
|         | Without noise                                | SNR=35 dB | Without noise                              | SNR=35 dB | Without noise                              | SNR=35 dB |
| 1       | 100.00                                       | 99.26     | 100.00                                     | 100.00    | 100.00                                     | 93.67     |
| 2       | 99.25  | 99.02     | 100.00                                     | 100.00    | 94.80                                      | 94.87     |
| 3       | 100.00                                       | 99.26     | 100.00                                     | 99.22     | 98.63                                      | 97.37     |
| 4       | 100.00                                       | 99.02     | 99.22                                      | 99.22     | 96.05                                      | 97.26     |
| 5       | 98.26  | 99.51     | 100.00                                     | 99.14     | 100.00                                     | 97.37     |
| Average | 99.50  | 99.13     | 99.84                                      | 99.52     | 97.90                                      | 96.11     |

Table III shows the performance against delayed islanding detection. Finally, the accuracy is defined as the ratio of the sum of islanding events and events predicted as non-islanding to the sum of both events and islanding events wrongly predicted as non-islanding. The overall accuracy in islanding classification is shown in Table IV. To make the stochastic optimization fair, five runs are considered, and the average performance of each metric is calculated. Moreover, the robustness of the proposed scheme is evaluated by introducing uncertainty to the training and testing data with an SNR value of 35 dB. The proposed IIDM is benchmarked with five-

cycle data, i.e., the data is used to extract the energy, and standard deviation of the time-frequency information in a test voltage signal is obtained for five cycles of observation period which represents 83.3 ms window width in power system of 60 Hz. It is worth mentioning that fast digital signal processing tools allow the reduction of computation time required for feature extraction from the test signal. During the offline simulation of the proposed scheme, the time required to test an unseen dataset of the GWO-ANN is shown in Table V.

TABLE III  
PERFORMANCE ANALYSIS OF PROPOSED IIDM AGAINST DELAYED DETECTION

| Run     | Dependability during islanding of multi-DERs (%) |           | Dependability during islanding of IVB DERs (%) |           | Dependability during islanding of SMB DERs (%) |           |
|---------|--|-----------|--|-----------|--|-----------|
|         | Without noise                                    | SNR=35 dB | Without noise                                  | SNR=35 dB | Without noise                                  | SNR=35 dB |
| 1       | 100.00   | 100.00    | 100.00   | 99.22     | 100.00   | 100.00    |
| 2       | 100.00   | 100.00    | 100.00   | 98.45     | 100.00   | 100.00    |
| 3       | 100.00   | 100.00    | 100.00   | 99.22     | 98.63  | 100.00    |
| 4       | 100.00   | 99.75     | 100.00   | 98.45     | 100.00   | 95.95     |
| 5       | 100.00   | 100.00    | 100.00   | 89.15     | 98.63  | 100.00    |
| Average | 100.00   | 99.95     | 100.00   | 96.90     | 99.45  | 99.19     |

TABLE IV  
OVERALL PERFORMANCE OF ACCURATE ISLANDING DISCRIMINATION FROM NON-ISLANDING EVENTS

| Run     | Accuracy during islanding of multi-DERs (%) |           | Accuracy during islanding of IVB DERs (%) |           | Accuracy during islanding of SMB DERs (%) |           |
|---------|---|-----------|---|-----------|---|-----------|
|         | Without noise                               | SNR=35 dB | Without noise                             | SNR=35 dB | Without noise                             | SNR=35 dB |
| 1       | 100.00                                      | 99.50     | 100.00                                    | 99.70     | 100.00                                    | 98.15     |
| 2       | 99.25                                       | 99.34     | 98.52                                     | 99.40     | 99.50                                     | 98.52     |
| 3       | 100.00                                      | 99.50     | 99.26                                     | 99.40     | 100.00                                    | 99.26     |
| 4       | 100.00                                      | 99.17     | 98.89                                     | 99.10     | 100.00                                    | 98.15     |
| 5       | 98.26                                       | 99.67     | 99.63                                     | 95.50     | 98.84                                     | 99.26     |
| Average | 99.50                                       | 99.44     | 99.26                                     | 98.62     | 99.67                                     | 98.67     |

TABLE V  
TESTING TIME OF GWO-ANN

| Run     | Testing time during islanding of multi-<br>DERs (s) |           | Testing time during islanding of IVB<br>DERs (s) |           | Testing time during islanding of SMB<br>DERs (s) |           |
|---------|---|-----------|--|-----------|--|-----------|
|         | Without noise                                       | SNR=35 dB | Without noise                                    | SNR=35 dB | Without noise                                    | SNR=35 dB |
| 1       | 0.0069  | 0.0067    | 0.0200   | 0.0245    | 0.0049   | 0.0054    |
| 2       | 0.0042  | 0.0033    | 0.0018   | 0.0024    | 0.0017   | 0.0022    |
| 3       | 0.0038  | 0.0032    | 0.0017   | 0.0020    | 0.0019   | 0.0029    |
| 4       | 0.0035  | 0.0034    | 0.0021   | 0.0023    | 0.0015   | 0.0016    |
| 5       | 0.0029  | 0.0034    | 0.0194   | 0.0025    | 0.0020   | 0.0015    |
| Average | 0.0426  | 0.0040    | 0.0090   | 0.0674    | 0.0024   | 0.0272    |

The detection time of islanding operation depends on the speed of digital signal processing and feature extraction, the testing time of the GWO-ANN classifier, and the size of the data. The proposed method has been simulated on an Intel® Core (TM) i5-2320 computer with 8 GB installed memory, running at 3 GHz.

Classical passive islanding detection schemes mainly depend on the voltage and frequency deviations monitored at the PoC of the targeted DER before and after the islanding event. The power variation obeys the following equations:

$$\Delta P = P_{DERs} + P_{maingrid} - P_{load} \quad (14)$$

$$\Delta Q = Q_{DERs} + Q_{maingrid} - Q_{load} \quad (15)$$

where  $P_{DERs}$ ,  $P_{maingrid}$ , and  $P_{load}$  are the active power of DERs, main grid, and loads, respectively; and  $Q_{DERs}$ ,  $Q_{maingrid}$ , and  $Q_{load}$  are the reactive power of DERs, main grid, and loads, respectively.

The voltage and frequency changes will be significant in unbalanced power between the generation and load, and eventually, islanding detection could be achieved using classical IDMs. However, as the penetration level of DERs increases, the relative variation due to loss of the main grid is negligible. Thus, islanding detection is not achieved using frequency and voltage relays. Unlike IDMs that depend on determining threshold values and face significant NDZ issues, the proposed IDM relies on statistical features, signatures of IMFs, and GWO-ANN classifier learning from data sets.

Based on this, the proposed IDM discriminates the events of unseen data without the problem of NDZ. To address the issue of NDZ, an active power imbalance of  $-50\%$  to  $50\%$  and reactive power imbalance of  $-20\%$  to  $20\%$  in the islanded system are considered. Furthermore, the islanding classification of the proposed IIDM is compared with the state-of-the-art techniques such as SVM and extreme learning machine (ELM) classifiers.

The performance comparison of SVM, ELM and proposed IIDM classifier is shown in Figs. 8-10, with constant features including the uncertainty.

The proposed IIDM shows better performance in detecting islanding and non-islanding conditions as compared to SVM and ELM for various datasets considering the islanding events of IVB, SMB, and multiple types of DERs.

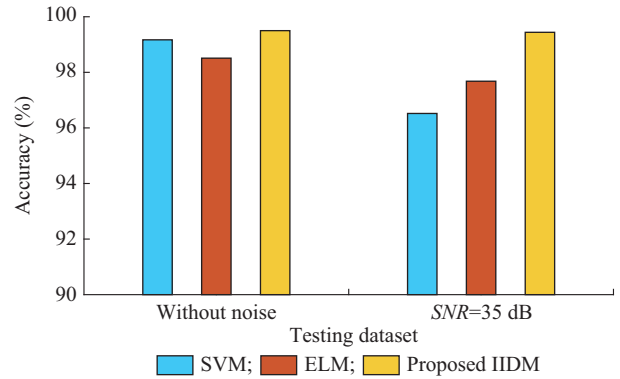


Fig. 8. Performance comparison of proposed IIDM with SVM and ELM during islanding of multi-DERs.

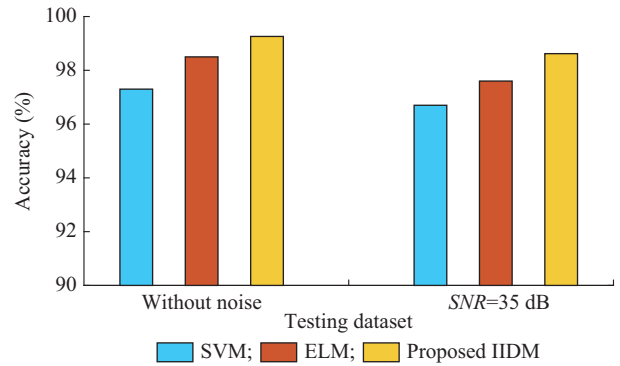


Fig. 9. Performance comparison of proposed IIDM with SVM and ELM during islanding of IVB DERs.

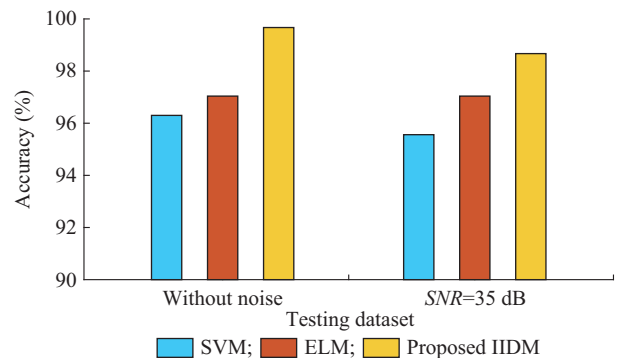


Fig. 10. Performance comparison of proposed IIDM with SVM and ELM during islanding of SMB DERs.



Moreover, compared to IDMs solely based on signal processing, one of the most important aspects of the proposed IIDM is that there is no need for any threshold values to differentiate between the islanding operation and other non-islanding events, even with zero power mismatch between the generation and load. Furthermore, the method is suitable for multiple types of DERs connected at multiple points in the distribution network.

## VI. CONCLUSION AND FUTURE WORKS

In this study, a GWO-ANN-based islanding detection using modal voltage IMF features is proposed. The proposed IIDM uses a hybrid VMD Hilbert transform technique for feature extraction, and then energy and standard deviation features are used to train and test the GWO-ANN model for identifying islanding events. It is capable of detecting islanding operation in multiple types of DERs integrated with the distribution network. The simulation results in MATLAB/Simulink environment show the efficacy of the proposed IIDM in terms of islanding classification accuracy, computation time, and robustness against noise conditions for the measured voltage signal. Moreover, the simulation results show that the accuracy of the proposed IIDM is higher than those of the SVM and the ELM classifiers. Further research studies need to explore the hardware in the loop (HIL) implementation of GWO-ANN for islanding detection and microgrid protection.

## REFERENCES

- [1] P. S. Georgilakis and N. D. Hatziaargyriou, "Optimal distributed generation placement in power distribution networks: models, methods, and future research," *IEEE Transactions on Power Systems*, vol. 28, no. 3, pp. 3420-3428, Jan. 2013.
- [2] V. C. Gungor, D. Sahin, K. Taskin *et al.*, "A survey on smart grid potential applications and communication requirements," *IEEE Transactions on Industrial Informatics*, vol. 9, no. 1, pp. 28-42, Feb. 2013.
- [3] A. Mohammadi and S. Bahrami, "An overview of future microgrids," in *Smart Microgrids*, Cham: Springer, 2019, pp. 1-6.
- [4] A. Sarwata, M. Amini, A. Domijan *et al.*, "Weather-based interruption prediction in the smart grid utilizing chronological data," *Journal of Modern Power Systems and Clean Energy*, vol. 4, no. 2, pp. 308-315, May 2016.
- [5] P. Dash, P. Malhar, and S. Barik, "Estimation of power quality indices in distributed generation systems during power islanding conditions," *International Journal of Electrical Power & Energy Systems*, vol. 36, no. 1, pp. 18-30, Mar. 2012.
- [6] J. Satish, R. Deepak, M. Ravindra *et al.*, "Likelihood of islanding in distributed feeders with photovoltaic generation," in *Proceedings of 2007 IEEE PES General Meeting*, Tampa, USA, Jun. 2007, pp. 1-6.
- [7] X. Liu, X. Zheng, Y. He *et al.*, "Passive islanding detection method for grid-connected inverters based on closed-loop frequency control," *Journal of Electrical Engineering Technology*, vol. 14, pp. 2323-2332, May 2019.
- [8] T. Basso, "IEEE 1547 and 2030 standards for distributed energy resources interconnection and interoperability with the electricity grid," National Renewable Energy Laboratory (NREL), Golden, USA, Dec. 2014.
- [9] *Inverters, Controllers and Interconnection System Equipment for Use with Distributed Energy Resources*, Standard UL-1741, Jan. 2010.
- [10] D. Soham, K. Pradip, B. Jaya *et al.*, "Shifting of research trends in islanding detection method - a comprehensive survey," *Protection and Control of Modern Power Systems*, vol. 3, no. 1, pp. 1-20, Jan. 2018.
- [11] Y. Shang, S. Shi, and X. Dong, "Islanding detection based on asymmetrical tripping of feeder circuit breaker in ungrounded power distribution system," *Journal of Modern Power Systems and Clean Energy*, vol. 3, no. 4, pp. 526-532, Oct. 2015.
- [12] A. Khamis, A. Shareef, E. Bizkevelci *et al.*, "A review of islanding detection techniques for renewable distributed generation systems," *Renewable and Sustainable Energy Reviews*, vol. 28, no. 1 pp. 483-493, Dec. 2013.
- [13] A. Timbus, A. Oudalov, and C. Ho, "Islanding detection in smart grids," in *Proceedings of 2010 IEEE Energy Conversion Congress and Exposition*, Atlanta, USA, Sept. 2010, pp. 1-7.
- [14] I. Balaguer, H. Kim, F. Peng *et al.*, "Survey of photovoltaic power systems islanding detection methods," in *Proceedings of 2008 34th Annual Conference of IEEE Industrial Electronics*, Orlando, USA, Nov. 2008, pp. 1-5.
- [15] L. Lopes and Y. Zhang, "Islanding detection assessment of multi-inverter systems with active frequency drifting methods," *IEEE Transactions on Power Delivery*, vol. 23, no. 1 pp. 480-486, Dec. 2007.
- [16] V. Menon and M. Nehrir, "A hybrid islanding detection using voltage unbalance and frequency set point," *IEEE Transactions on Power Systems*, vol. 22, no. 1, pp. 442-448, Jan. 2007.
- [17] F. Mango, M. Liserre, A. Dell'Aquila *et al.*, "Overview of anti-islanding algorithms for PV systems, Part i: passive methods," in *Proceedings of 2006 12th International Power Electronics and Motion Control Conference*, Portoroz, Slovenia, Aug.-Sept. 2006, pp. 1-5.
- [18] H. Zeineldin and H. Kirtley, "Performance of the OVP/UPV and OFP/UPF method with voltage and frequency-dependent loads," *IEEE Transactions on Power Delivery*, vol. 24, no. 2, pp. 772-778, Mar. 2009.
- [19] P. Mahat, Z. Chen, and B. Bak-Jensen, "A hybrid islanding detection technique using average rate of voltage change and real power shift," *IEEE Transactions on Power Systems*, vol. 24, no. 2, pp. 764-771, Mar. 2009.
- [20] J. Yin, C. Diduch, and L. Chang, "Islanding detection using proportional power spectral density," *IEEE Transactions on Power Delivery*, vol. 23, no. 2, pp. 776-784, Mar. 2008.
- [21] S. Samantaray, A. Samui, and A. Babu, "Time-frequency transform-based islanding detection in distributed generation," *IET Renewable Power Generation*, vol. 5, no. 6, pp. 431-438, Dec. 2011.
- [22] P. Pigazo, M. Liserre, R. Mastromauro *et al.*, "Wavelet-based islanding detection in grid-connected PV systems," *IEEE Transactions on Industrial Electronics*, vol. 56, no. 11, pp. 4445-4455, Nov. 2009.
- [23] H. Do, X. Zhang, N. Nguyen *et al.*, "Passive-islanding detection method using the wavelet packet transform in grid-connected photovoltaic systems," *IEEE Transactions on Power Electronics*, vol. 31, no. 10, pp. 6955-6967, Oct. 2016.
- [24] N. Mohammadzadeh and S. Afsharnia, "A new passive islanding detection method and its performance evaluation for multi-DG systems," *Electric Power Systems Research*, vol. 110, pp. 180-187, May 2014.
- [25] B. Matic-Cuka and M. Kezunovic, "Islanding detection for inverter-based distributed generation using support vector machine method," *IEEE Transactions on Smart Grid*, vol. 5, no. 6, pp. 2676-2686, Nov. 2014.
- [26] V. Merline, R. Santos, A. Grilo *et al.*, "A new artificial neural network-based method for islanding distributed generators," *International Journal of Electrical Power & Energy Systems*, vol. 75, pp. 139-151, Feb. 2016.
- [27] K. Susmita and R. Subhransu, "Data-mining-based intelligent anti-islanding protection relay for distributed generations," *IET Generation Transmission & Distribution*, vol. 8, no. 4, pp. 629-639, Apr. 2014.
- [28] R. Haider, C. Kim, T. Ghanbari *et al.*, "Passive islanding detection scheme based on autocorrelation function of modal current envelope for photovoltaic units," *IET Generation, Transmission & Distribution*, vol. 12, no. 3, pp. 726-736, Feb. 2018.
- [29] N. Perera, A. Rajapakse, and T. Buchholzer, "Isolation of faults in distribution networks with distributed generators," *IEEE Transactions on Power Delivery*, vol. 23, no. 4, pp. 2347-2355, Sept. 2008.
- [30] S. Admasie, S. B. Bukhari, R. Haider *et al.*, "A passive islanding detection scheme using variational mode decomposition based-mode singular entropy for integrated microgrids," *Electric Power Systems Research*, vol. 177, pp. 1-12, Dec. 2019.
- [31] K. Dragomiretskiy and Z. Dominique, "Variational mode decomposition," *IEEE Transactions on Signal Processing*, vol. 62, no. 3, pp. 531-544, Nov. 2013.
- [32] M. Mishra and K. Pravat, "Detection and classification of micro-grid faults based on HHT and machine learning techniques," *IET Generation, Transmission & Distribution*, vol. 12, no. 2, pp. 388-397, Feb. 2018.
- [33] D. Camarena-Martinez, M. Valtierra-Rodriguez, C. A. Perez-Ramirez *et al.*, "Novel downsampling empirical mode decomposition approach for power quality analysis," *IEEE Transactions on Industrial Electronics*, vol. 63, no. 4, pp. 2369-2378, Dec. 2015.

- [34] Z. Wang, "Hilbert transform applications in signal analysis and non-parametric identification of linear and nonlinear systems," Ph.D. dissertation, Department of Civil, Architectural and Environmental Engineering, Missouri University of Science and Technology, Rolla, USA, 2011.
- [35] T. Wang, Y. He, B. Li *et al.*, "Fault diagnosis of transformer based on self powered RFID sensor tag and improved HHT," *Journal of Electrical Engineering Technology*, vol. 13, no. 5, pp. 2134-2143, Sept. 2018.
- [36] J. Zhang, L. Xiao, K. Chen *et al.*, "Classification of power quality disturbances via deep learning," *IETE Technical Review*, vol. 34, no. 4, pp. 408-415, Jul. 2016.
- [37] S. Khokhar, Z. Mohd, A. Memon *et al.*, "A new optimal feature selection algorithm for classification of power quality disturbances using discrete wavelet transform and probabilistic neural network," *Measurement*, vol. 95, no. 1, pp. 246-259, Jan. 2017.
- [38] S. Mirjalili, S. Z. Mohd Hashim, and H. M. Sardroudi, "Training feed-forward neural networks using hybrid particle swarm optimization and gravitational search algorithm," *Applied Mathematics and Computation*, vol. 218, no. 22, pp. 11125-11137, Jul. 2012.
- [39] D. Whitley, T. Starkweather, and C. Bogart, "Genetic algorithms and neural networks: optimizing connections and connectivity," *Parallel Computing*, vol. 14, no. 3, pp. 347-361, Aug. 1990.
- [40] D. Karaboga, B. Akay, and C. Ozturk, "Artificial bee colony (ABC) optimization algorithm for training feed-forward neural networks," in V. Torra, Y. Narukawa, and Y. Yoshida (Eds.), *Modeling Decisions for Artificial Intelligence*, Berlin: Springer, 2007, pp. 318-329.
- [41] S. Mirjalili, "How effective is the grey wolf optimizer in training multi-layer perceptrons," *Applied Intelligence*, vol. 43, no. 1, pp. 150-161, Jan. 2015.
- [42] S. Mirjalili, M. Mirjalili, and A. Lewis, "Grey wolf optimizer," *Advances in Engineering Software*, vol. 69, pp. 46-61, Mar. 2014.
- [43] H. Faris, I. Aljarah, M. Al-Betar *et al.*, "Grey wolf optimizer: a review of recent variants and applications," *Neural Computing and Applications*, vol. 30, no. 20, pp. 413-435, Jul. 2018.
- [44] M. Mishra, M. Sahani, and P. K. Rout, "An islanding detection algorithm for distributed generation based on Hilbert-Huang transform and extreme learning machine," *Sustainable Energy, Grids and Networks*, vol. 9, pp. 13-26, Mar. 2017.

**Samuel Admasie** received the B.Sc. degree in electrical engineering from Addis Ababa Institute of Technology, Addis Ababa, Ethiopia in 2015. Currently, he is working towards the Ph.D. degree in Sungkyunkwan University,

Suwon, South Korea. His research interests include DER integration, artificial intelligence applications for power system protection and islanding detection, and distribution system planning.

**Syed Basit Ali** received the B.Sc. degree in electrical engineering from University of Azad Jammu and Kashmir, Muzaffarabad, Pakistan in 2011, the M.Sc. degree in electrical engineering from University of Engineering and Technology, Taxila, Pakistan in 2014, and the Ph.D. degree in electrical engineering from Sungkyunkwan University, Suwon, South Korea, in 2019. Currently, he is working as an Assistant Professor with the US-Pakistan Center for Advanced Studies in Energy, National University of Sciences and Technology, Islamabad, Pakistan. His current research interests include power system protection, artificial intelligence applications for protection and control, microgrid, and islanding detection.

**Teke Gush** received the B.Sc. degree in electrical engineering from Addis Ababa Institute of Technology, Addis Ababa, Ethiopia in 2015. He is currently working toward the Ph.D. degree in Sungkyunkwan University, Suwon, South Korea. His research interests include renewable energy grid integration, power system protection, artificial intelligence applications for protection of microgrid and islanding detection.

**Raza Haider** received his B.E degree from Balochistan University of Engineering and Technology, Khuzdar, Pakistan, the M.E degree from Mehran University of Jamshoro, Sindih, Pakistan, and the Ph.D. degree from Sungkyunkwan University, Suwon, South Korea in 2003, 2009, and 2019, respectively, in the field of electrical engineering. Currently, he is working as Associate Professor in the Department of Electrical Engineering, Balochistan University of Engineering and Technology, Khuzdar, Pakistan. His research interests include power systems, microgrid protection, and distribution generation.

**Chul Hwan Kim** received the B.S., M.S., and Ph.D. degrees in electrical engineering from Sungkyunkwan University, Suwon, South Korea in 1982, 1984, and 1990, respectively. In 1990, he joined Cheju National University, Cheju, South Korea, as a Full-Time Lecturer. He was a Visiting Academic at the University of Bath, Bath, UK, in 1996, 1998, and 1999, respectively. He has been a Professor in the College of Information and Communication Engineering, Sungkyunkwan University, since 1992. Currently, he is a Director with the Center for Power It (CPIT) in Sungkyunkwan University. His research interests include power system protection, artificial-intelligence applications for protection and control, modeling and protection of underground cable, and Electromagnetic Transients Program software.